Electronic Supplementary Material (ESI) for Chemical Science.

Supporting Information

Revealing the role of nitroxyl during hepatic ischemia-reperfusion injury with a NIR-II luminescent nanoprobe

Chenchen Li,[‡] Wenqiang Bi,[‡] Tao Liang, Zhen Li,* and Zhihong Liu*

College of Health Science and Engineering, College of Chemistry and Chemical Engineering, Hubei University, Wuhan 430062, China

[‡]C. Li and W. Bi contributed equally to this work.

Materials and apparatus

2-(Diphenylphosphino)benzoic acid (DPPBac), DMAP, NaAc, 1-octadecene (ODE), oleic acid (OA) and $LnCl_3 \cdot 6H_2O$ were obtained from Aladdin Reagent, Ltd. (Shanghai, China). EDC was provided by Sigma-Aldrich. Angeli's salt (AS) was obtained from Cayman Chemical. DSPE-PEG_{2000} was purchased from Xi'an ruixi Biological Technology Co., Ltd. Other chemical reagents were obtained from Sinopharm Chemical Reagent Co., Ltd. (Shanghai, China). The reagents were all analytical or higher grade and used without further purification. All aqueous solutions were prepared using ultrapure water (Mill-Q, Millipore, 18.2 MΩ resistivity). The size and morphology of RENPs were characterized by a JEM-2010 transmission electron microscope (TEM) with an acceleration voltage of 200 kV. FTIR spectra were acquired using a Nicolet 5700 FTIR Spectrometer (Thermo Fisher Scientific, USA) with the KBr pellet technique. The crystal phase of nanoparticles was characterized by an X-ray diffractometer (XRD, Bruker D8 Discover) with a 2θ range from 10° to 80° with Cu Kα irradiation (k=1.5406 Å). NIR-II fluorescence spectra were excited by 808-nm or 980-nm laser and measured with a fluorometer (FLS1000, Edinburgh Instrument). UV-vis spectra were recorded by a UV 2550 UV-vis spectrophotometer (Shimadzu, Japan). Fluorescence microscopy images of HepG2 cells were conducted on Zeiss LSM 880 Microscope. *In vivo* NIR-II luminescence images were acquired by *In-Vivo* Master NIR-II luminescence imaging system (Grand Imaging Technology Co. Ltd., Wuhan).

Synthesis of Cy-TP

The synthetic routine of Cy-TP was shown in Figure S29. Compound 1-6 were synthesized as reported.[1-3] DPPBac (30 mg, 1 mmol), EDC (21 mg, 1 mmol) and DMAP (10 mg, 0.5 mmol) were dissolved in CH_2Cl_2 and stirred in ice water for 30 min. Then compound 6 was added into the reaction system and stirred overnight at room temperature. After the reaction, green solid was obtained by column

chromatography. ^{1}H NMR (400 MHz, DMSO, Figure S30) δ 8.72-8.63 (m, 1H), 7.87-7.77 (m, 2H), 7.65 (d, *J* = 14.1 Hz, 2H), 7.56 (d, *J* = 7.4 Hz, 2H), 7.40 (d, *J* = 3.2 Hz, 4H), 7.37-7.28 (m, 6H), 7.25-7.18 (m, 2H), 7.11-7.04 (m, 5H), 6.21 (d, *J* = 14.2 Hz, 2H), 4.16 (t, *J* = 6.5 Hz, 4H), 3.99 (t, *J* = 6.6 Hz, 4H), 2.68 (s, 4H), 2.25 (t, *J* = 7.3 Hz, 4H), 1.88 (s, 2H), 1.70 (dd, *J* = 13.4, 6.6 Hz, 4H), 1.54-1.48 (m, 8H), 1.44-1.25 (m, 28H), 1.23 (s, 12H), 0.86 (t, *J* = 7.4 Hz, 6H). ^{13}C NMR (101 MHz, DMSO, Figure S31) δ 173.36, 171.91, 163.47, 159.06, 142.48, 141.36, 139.77, 137.63, 137.52, 13.5.36, 134.99, 133.78, 133.58, 131.38, 131.19, 130.09, 129.32, 129.26, 129.19, 129.01, 125.45, 123.04, 121.32, 111.81, 101.33, 63.78, 49.11, 44.05, 33.98, 31.61, 30.68, 30.29, 29.49, 29.23, 29.08, 28.89, 27.84, 27.29, 26.50, 24.95, 24.15, 22.57, 20.98, 19.09, 14.41, 13.99. HRMS (m/z, Figure S32): $[M]^+$ calcd for $[C_{79}H_{102}N_2O_6P]^+$ 1205.7470, found 1205.7463.

Synthesis of $NaYF_4$:Yb,Er,Ce@$NaYF_4$:Nd core-shell nanoparticles

Core-shell RENPs were prepared by seed-mediated growth method. First, 0.75 mmol Ln(oleate)$_3$ (Y^{3+}: Yb^{3+}: Er^{3+}: Ce^{3+}= 73: 20: 2: 5) and 20 mmol NaF were added into the mixed solvent of 20 mL of OA and ODE in a three-necked flask. After vacuuming, the mixture was kept in argon atmosphere at 110°C for 1 h. Then the temperature was raised to 320°C and kept under the protection of argon for 75 min. 4 ml of the reaction mixture was removed and stored for characterization. Ln(oleate)$_3$ dissolved in 8 mL of OA/ODE (0.4 mmol, Y^{3+}: Nd^{3+} = 4: 1) was added and stirred at 320°C for 40 min. When the mixture cooled to room temperature, an equal amount of ethanol was added to precipitate the nanoparticles. The nanoparticles were centrifuged and washed three times with 1:1 hexane/ethanol. Finally, the obtained OA-RENPs were dispersed in hexane for use.

Preparation of Cy-TP-RENPs

1 mg/mL OA-RENPs and the same amount of DSPE-PEG_{2000} were dissolved in chloroform. The mixture was kept stirring overnight until the chloroform was completely volatilized, then the residue (named RENPs-DSPE-PEG_{2000}) was dispersed in ultra-pure water. Different volumes of Cy-TP dissolved in dimethyl sulfoxide (DMSO) were slowly dropped into RENPs-DSPE-PEG_{2000} solution and shaken vigorously for about 3 minutes until completely mixed. The mixture was centrifuged to remove excess DSPE-PEG_{2000} and Cy-TP. The precipitation was washed twice with ultrapure water and dispersed into ultrapure water with the final concentration of 1 mg/mL. The final product was Cy-TP-RENPs.

Measurement of loading capacity of Cy-TP

Cy-TP-RENPs was divided into two equal parts and centrifuged to obtain the precipitate, which were then dispersed in equal volume of H_2O and DMSO, respectively. The hydrophobic layer of Cy-TP-RENPs was dissociated in DMSO and the loaded Cy-TP was finally dispersed in DMSO. The absorption spectra of Cy-TP-RENPs in different media were measured and denoted as $A_{hydrophobic\ layer}$ and A_{DMSO}. The loading capacity of Cy-TP for RENPs was calculated by the following equations:

$$\frac{Abs._{hydrophobic\ layer}}{Abs._{DMSO}} = \frac{\varepsilon_{hydrophobic\ layer}}{\varepsilon_{DMSO}} \quad (1)$$

$$X = \frac{Abs._{hydrophobic\ layer}}{\varepsilon_{hydrophobic\ layer}\, M_{RENPs}} \quad (2)$$

where $\varepsilon_{hydrophobic\ layer}$ and ε_{DMSO} are the molar absorption coefficients of Cy-TP in hydrophobic layer and DMSO, respectively. The value of ε_{DMSO} was acquired from Figure S3B, C. The average ratio value of $Abs._{hydrophobic\ layer}/Abs._{DMSO}$ was obtained from Figure S3D and $\varepsilon_{hydrophobic\ layer}$ can be calculated by equation (1). After that, the loading

capacity of Cy-TP, *X*, can be obtained according to equation (2). M_{RENPs} is the mass concentration of RENPs.

Determination of HNO in solution

Different concentrations of AS were added to Tris-HCl solution (100 mM, pH = 7.4) containing Cy-TP-RENPs (0.02 mg/mL). The mixture was incubated at 37°C for 30 min, and NIR-II luminescence intensity at 1550 nm excited by 980 and 808-nm laser was measured. The power density of both 980-nm and 808-nm lasers was 2.5 W/cm^2.

Stability of Cy-TP-RENPs and Cy-HNO-RENPs

Cy-HNO-RENPs were obtained by reacting Cy-TP-RENPs with 100 μM AS at 37°C in different media (Tris-HCl, DMEM, FBS), and NIR-II luminescence intensity was recorded at given intervals to study the thermodynamic stability. In addition, Cy-TP-RENPs and Cy-HNO-RENPs were incubated in buffers with different pH and NIR-II luminescence intensity was recorded.

Cell culture

HepG2 cells were cultured in a 96-well plate or a 35-nm glass plate in Dulbecco's modified Eagle's medium (MEM) supplemented with 10% fetal bovine serum (FBS), 1% penicillin, 1% streptomycin and 1% NEAA at 37°C in 5% CO_2 atmosphere.

Cytotoxicity of Cy-TP-RENPs

Cell counting kit-8 (CCK-8) assay was used to estimate the cytotoxicity of Cy-TP-RENPs with HepG2 cells. First, HepG2 cells were cultured in 96-well plates with MEM at 37°C and 5% CO_2 for 24 h. After adding different concentrations of Cy-TP-RENPs (0-0.6 mg/mL) into fresh MEM medium, the cells were cultured for another 24 h. Then, cells were washed with buffer and incubated with 0.5 mg/mL CCK-8 reagent at 37°C for 1

h. The absorbance at 450 nm was measured by a microplate reader. Cell viability was calculated by comparing the average absorbance of Cy-TP-RENPs-treated cells to control cells. The experiment was repeated six times for each concentration.

For Calcein-AM and PI costaining, HepG2 cells were treated with the mixture of PI (4.5 μM) and Calcein-AM (2 μM) and incubated at 37°C for 30 min. The confocal microscopy images of the cells were acquired by a confocal laser scanning microscope. The excitation wavelengths were 488 and 561 nm for Calcein-AM and PI, respectively, and the corresponding emissions were collected in the range of 500-550 and 580-650 nm.

***In vivo* toxicity**

All experimental procedures were performed in accordance with institutional animal care guidelines. The animal research committee of Hubei University approved all procedures involved in animal experiments. Healthy mice were intravenously injected with Cy-TP-RENPs (0, 5, 10 mg/100 g body weight) for 7 days (n = 3), the blood and major organs (heart, liver, spleen, lungs and kidneys) were taken for biochemical analysis and H&E staining.

***In vivo* NIR-II imaging of HNO in living mice**

The mice were divided into five groups and treated differently. The first group of mice was given an intraperitoneally (i.p.) injection of PBS. The second group of mice was i.p. injected with glutathione (GSH, 2 mM in saline, 200 μL) for 1 h. The third group of mice was i.p. injected with AS (25 μg/100 g body weight) for 1 h before imaging. The fourth group of mice was i.p. injected with AS (62.5 μg/100 g body weight) for 1 h before imaging. The fifth group of mice was given an i.p. injection of GSH (2 mM in saline, 200 μL) for 1 h followed by i.p. injection of AS (62.5 μg/100 g body weight). All the mice were intravenously (i.v.) injected with Cy-TP-RENPs (10 mg/mL, 100 μL) for 3

h before imaging. The *In-Vivo* Master NIR-II luminescence imaging system equipped with 808 and 980-nm laser and 1300 nm LP filter (90 mW/cm^2 power density, 300 ms exposure time) was used for NIR-II luminescence imaging.

***In vivo* NIR-II imaging of HNO in APAP-induced liver injury**

Balb/c mice (female, 20 ± 2 g, n = 3) were i.p. injected with different dosages of APAP (0, 10, 20 mg/100 g body weight). After stimulation for 12 h, Cy-TP-RENPs (10 mg/mL, 100 μL) were i.v. injected into the mice. After 3 h, the *In-Vivo* Master NIR-II luminescence imaging system equipped with 808 and 980-nm laser and 1300 nm LP filter (90 mW/cm^2 power density, 300 ms exposure time) was used for NIR-II luminescence imaging. For another group of mice, α-LA (5 mg/100 g body weight) was i.p. injected for 12 h before APAP stimulation.

***In vivo* NIR-II imaging of HNO in hepatic ischemia-reperfusion injury mouse model**

The hepatic ischemia-reperfusion injury mouse model was established according to the previous report.[4] Balb/c mice (female, 20 ± 2 g) were randomly divided into four groups (n = 5), namely, the sham group, the 30-min ischemia group, the 60-min ischemia group and the 90-min ischemia group. The mice in the sham group were given a midline laparotomy surgery without ischemia. The mice in the ischemia group were given a midline laparotomy surgery, and ischemia was induced by clamping the hepatic artery and portal vein for 30, 60, 90 min. After ischemia, the clamp was removed, followed by suturing the abdominal cavity layer by layer and reperfusion for 24 h. For the mice model with different times of reperfusion, Balb/c mice (female, 20 ± 2 g) with 30, 60 or 90-min ischemia were randomly divided into five groups, namely, the sham group (n = 5), the 3, 6, 12 or 20 h reperfusion group (n = 5). The mice in the sham group were given a midline laparotomy surgery without ischemia. The mice in the ischemia group were given a midline laparotomy surgery, and ischemia was

induced by clamping the hepatic artery and portal vein for 30, 60 or 90 min. After ischemia, the clamp was removed, followed by suturing the abdominal cavity layer by layer and then reperfusion for 3, 6, 12 or 20 h. Finally, *In-Vivo* NIR-II luminescence imaging was performed after administration of Cy-TP-RENPs (10 mg/mL, 100 μL), by using an *In-Vivo* Master NIR-II luminescence imaging system equipped with 808 and 980-nm excitation and 1300 nm LP filter. (90 mW/cm^2 power density, 300 ms exposure time).

Effect of HNO in hepatic ischemia-reperfusion injury mouse model

Balb/c mice were divided into four groups (n = 5). Group a was the sham group. In group b, the hepatic artery and portal vein were clipped for 90 min followed by reperfusion for 24 h. Group c and d were pretreated by i.p. injection with 50 μg/100 g body weight and 100 μg/100 g body weight of AS for 1 h, respectively. Then the hepatic artery and portal vein were clipped for 90 min followed by reperfusion for 24 h. All the mice were i.v. injected with Cy-TP-RENPs (10 mg/mL, 100 μL) for 3 h. The *In-Vivo* Master NIR-II luminescence imaging system equipped with 808 and 980-nm laser and 1300 nm LP filter (90 mW/cm^2 power density, 300 ms exposure time) was used for NIR-II luminescence imaging.

RNA-seq and data analysis

Total RNA was extracted from mice liver tissue in sham, IR, HNO-IR group, respectively. The transcriptome sequencing and analysis were conducted by BMKCloud (www.biocloud.net). Eukaryotic mRNA was enriched with magnetic beads with Oligo (dT), and then the mRNA was randomly interrupted by Fragmentation Buffer. The first and second cDNA strands were synthesized using mRNA as template, and the cDNA libraries are enriched by PCR. The Q-PCR method was used to accurately quantify the effective concentration of libraries to ensure the quality of libraries. Illumina

NovaSeq6000 platform was used for sequencing after qualifying database inspection. DESeq2 was used to test the statistical enrichment of differentially expressed genes in KEGG pathways. Genes with significant expression change was defined as standard of Fold Change≥2 and FDR<0.05.

Statistical analysis

All experiments were repeated at least three times. All data are presented as mean values ± SD. The differences of different groups were compared by two-tailed and unpaired t-test. Statistical significance was set at *P < 0.05, **P < 0.01, ***P < 0.001, and ****p<0.0001. Origin 2018, Graphpad Prism 9.0 and ImageJ were used to analyze the acquired data.

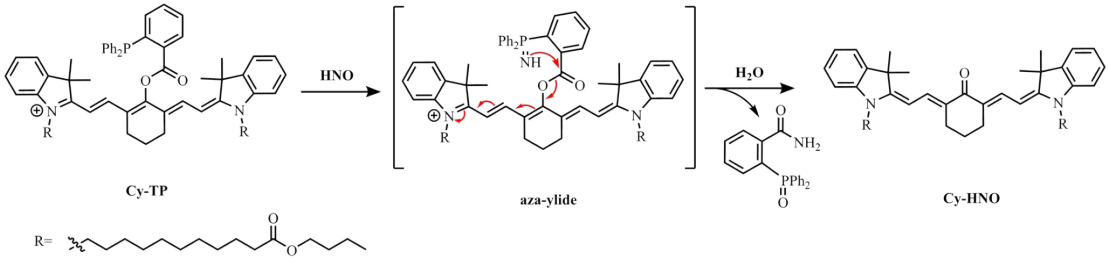

Figure S1. The response mechanism of Cy-TP toward HNO.

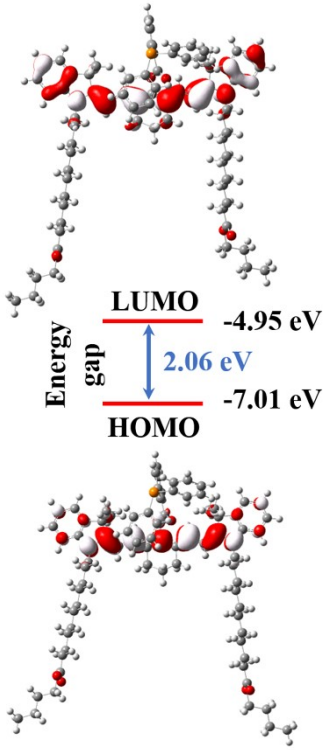

Figure S2. DFT-calculation result of Cy-TP.

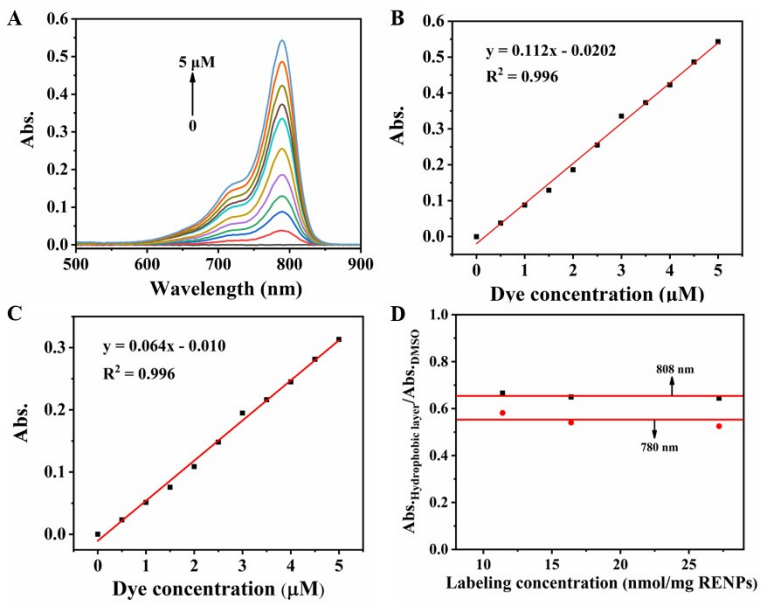

Figure S3. (A) The absorption spectra of Cy-TP with different concentration. The molar absorption coefficient of Cy-TP at 780 nm (B) and 808 nm (C). (D) The ratio of the absorbance of Cy-TP loaded in the hydrophobic layer to that of the equal amount of Cy-TP dissolved in DMSO. The average ratio at 780 and 808 nm were 0.55 and 0.65, respectively. The molar absorption coefficients of Cy-TP at 780 and 808 nm in hydrophobic layer were 6.16×10^4 and 4.16×10^4, respectively.

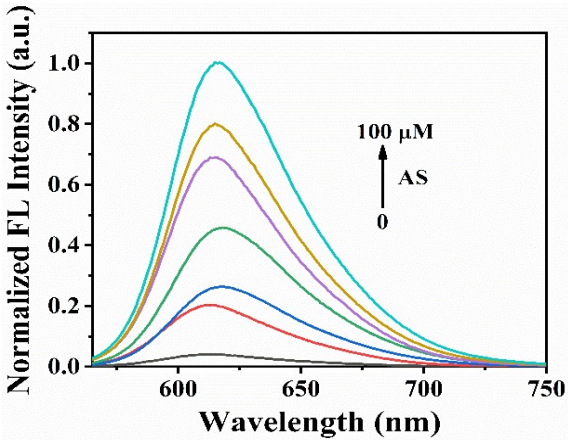

Figure S4. Emission spectra of Cy-TP under 550-nm excitation after responding to different concentrations of HNO.

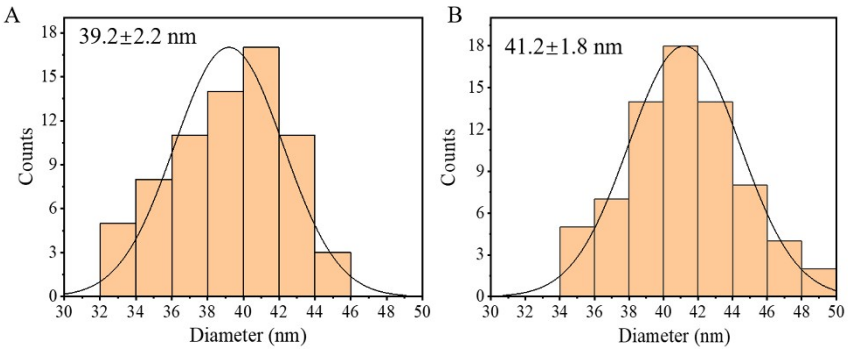

Figure S5. Histograms of the size distribution for (A) $NaYF_4$:20%Yb,2%Er,5%Ce, (B) $NaYF_4$:20%Yb,2%Er,5%Ce@$NaYF_4$:Nd.

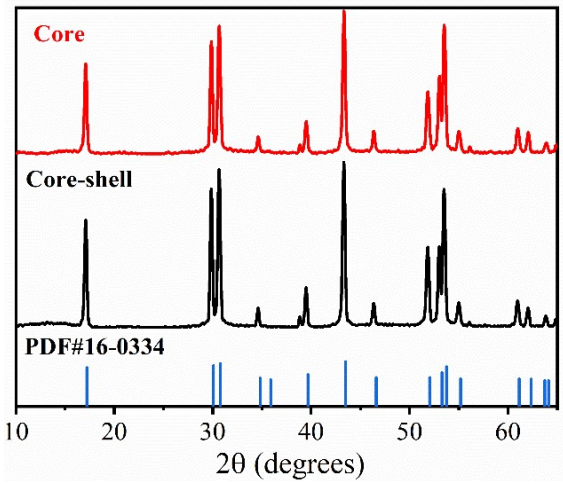

Figure S6. XRD patterns of core and core-shell structured RENPs.

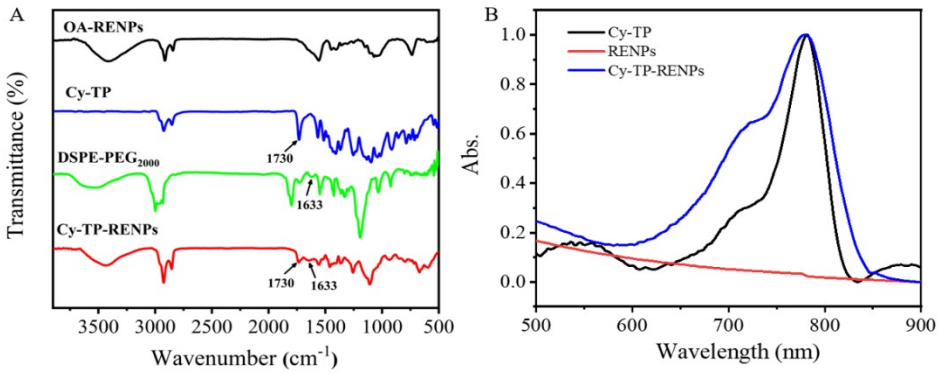

Figure S7. (A) FTIR spectra of OA-RENPs, Cy-TP, DSPE-PEG_{2000} and Cy-TP-RENPs. (B) UV-vis absorption spectra of Cy-TP, RENPs, and Cy-TP-RENPs in the Tris-HCl buffer (pH=7.4, 100 mM).

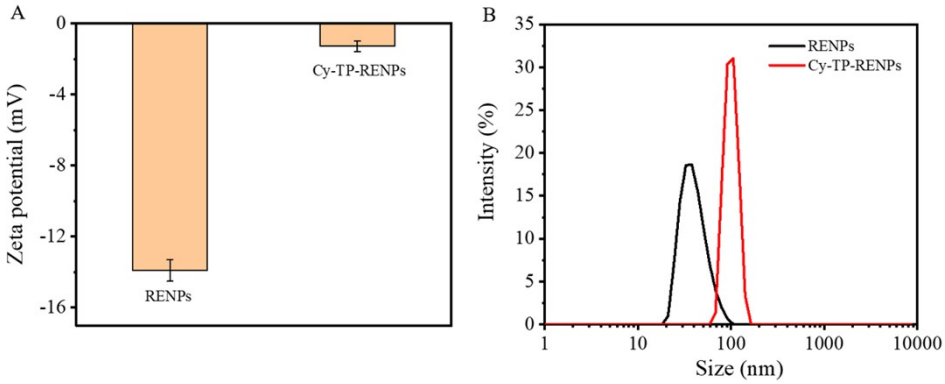

Figure S8. Zeta potential (A) and hydrodynamic diameter (B) of RENPs and Cy-TP-RENPs.

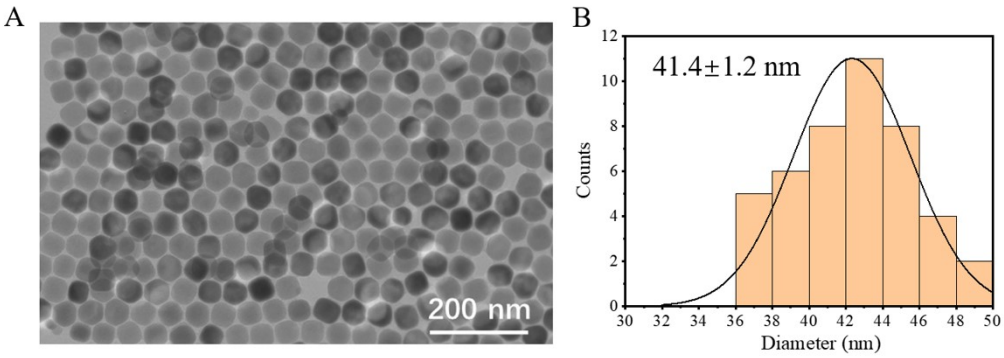

Figure S9. TEM image (A) and histograms of the size distribution (B) of Cy-TP-RENPs.

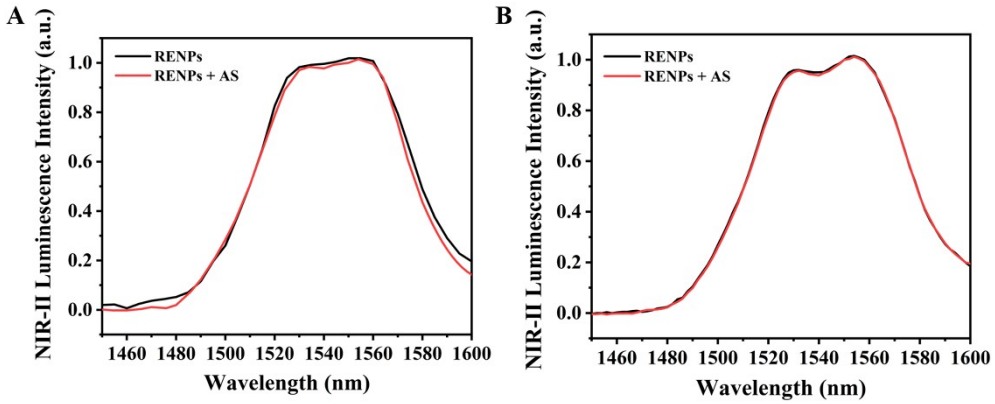

Figure S10. Emission spectra of RENPs under 808-nm excitation (A) and 980-nm excitation (B) after incubating to HNO.

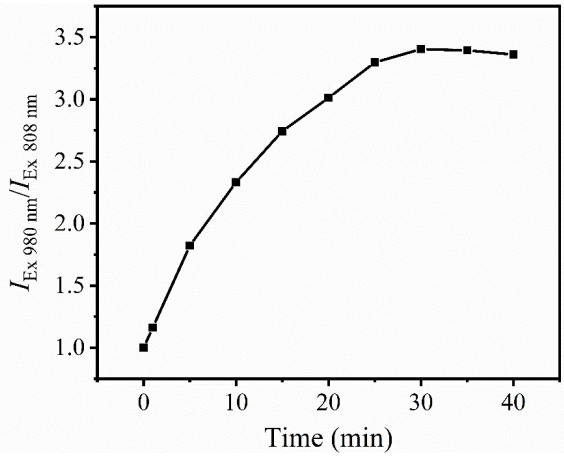

Figure S11. Dependence of the normalized ratio value ($I_{Ex\ 980\ nm}/I_{Ex\ 808\ nm}$) of Cy-TP-RENPs (0.02 mg/mL) on the time of the reaction with HNO (100 μM).

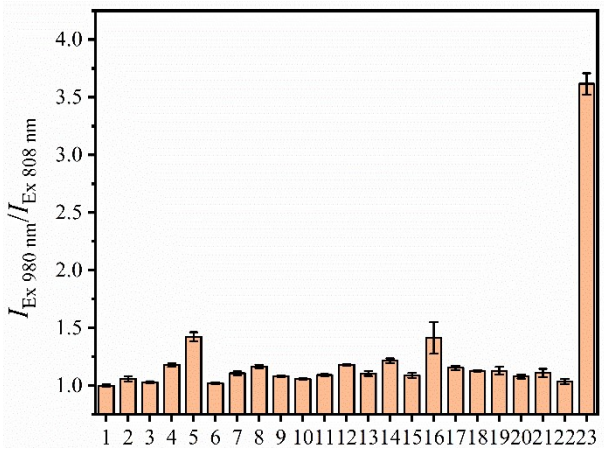

Figure S12. Selectivity of Cy-TP-RENPs (0.02 mg/mL) to HNO against other disruptors. The concentration of both HNO and other substances was 200 μM. (1: blank; 2: NaCl; 3: Fe^{2+}; 4: KCl; 5: Cu^{2+}; 6: Glucose; 7: BSA; 8: H_2O_2; 9: HClO; 10: ·OH; 11: $^1O_2$; 12: $O_2^{\bullet-}$; 13: Hcy; 14: GSH; 15: Cys; 16: NO_2^-; 17: $ONOO^-$; 18: NO; 19: NaHS; 20: Na_2SO_4; 21: $Na_2S_2O_3$; 22: H_2S_n; 23: HNO).

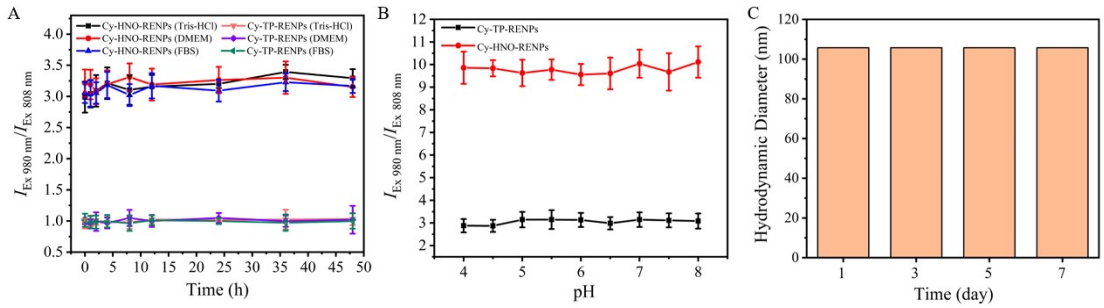

Figure S13. (A) Stability of Cy-TP-RENPs and the reaction product, Cy-HNO-RENPs, in different media including Tris-HCl, DMEM, FBS. (B) Stability of Cy-TP-RENPs and Cy-HNO-RENPs in buffer solution with different pH. (C) Hydrodynamic diameter of Cy-TP-RENPs measured by dynamic light scattering after incubation for different time in an aqueous solution (Tris-HCl, pH 7.4).

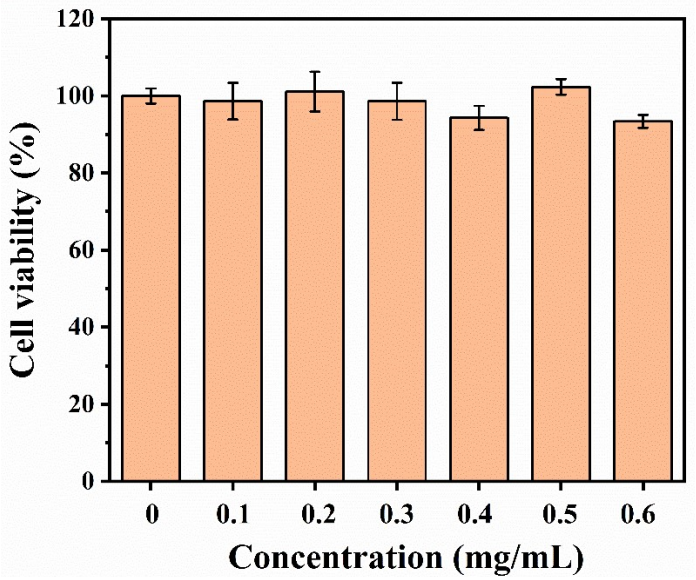

Figure S14. Cell viability of HepG2 cells incubated with different concentrations of Cy-TP-RENPs at 37°C for 24 h.

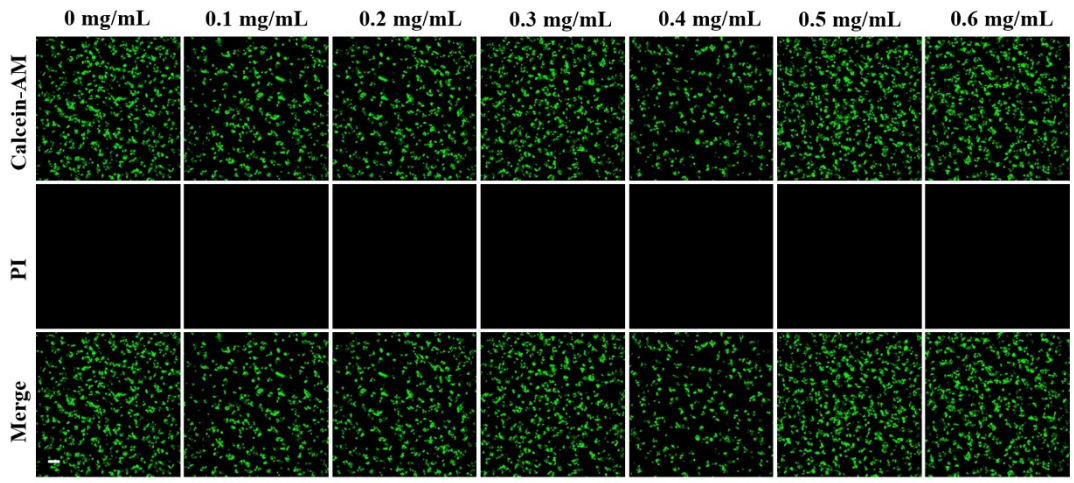

Figure S15. Confocal images of HepG2 cells incubated with different concentrations of Cy-TP-RENPs at 37°C for 24 h after co-staining with Calcein-AM and PI. Scale bar: 100 μm.

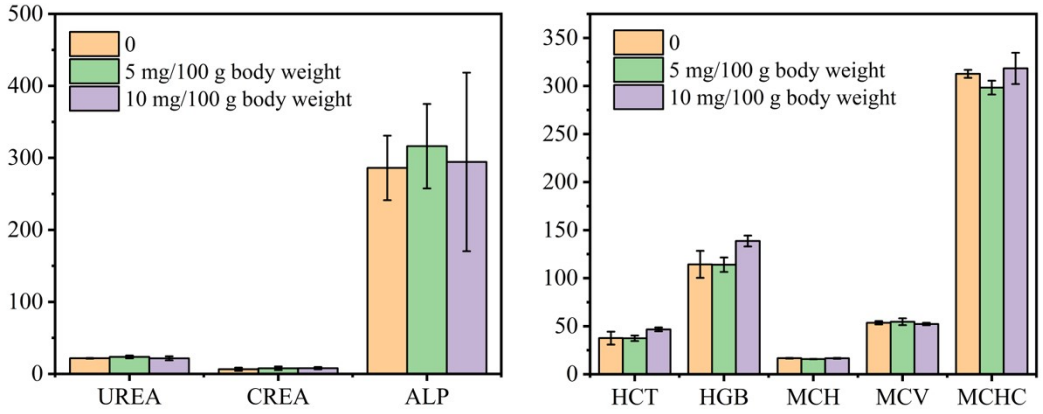

Figure S16. Blood routine and serum biochemical levels of mice after injecting different doses of Cy-TP-RENPs including UREA (μmol/L), creatinine (CREA: μmol/L), alkaline phosphatase (ALP: U/L), hematocrit (HCT: %), hemoglobin (HGB: g/L), mean corpuscular hemoglobin (MCH: pg), mean corpuscular volume (MCV: fL) and mean corpuscular hemoglobin concentration (MCHC: g/L).

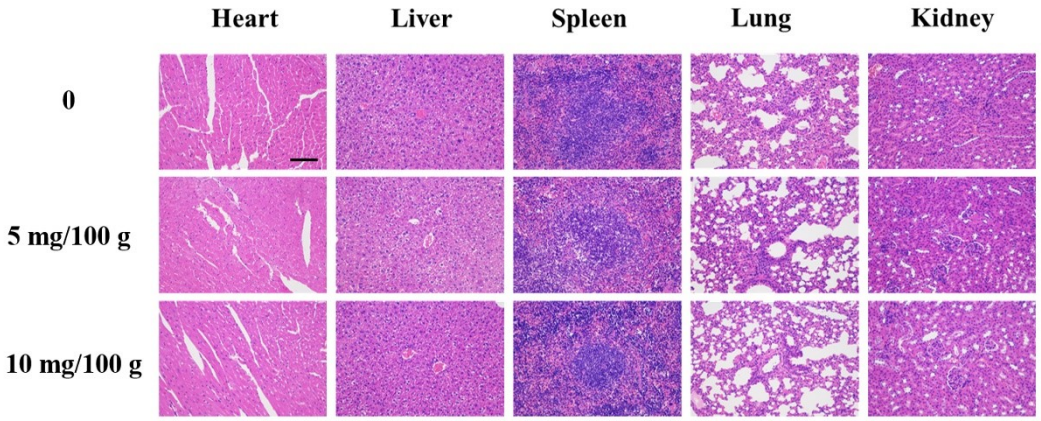

Figure S17. H&E staining images of major mice organs after intravenous injection of different dosages of Cy-TP-RENPs for 7 days. Scale bar: 100 μm.

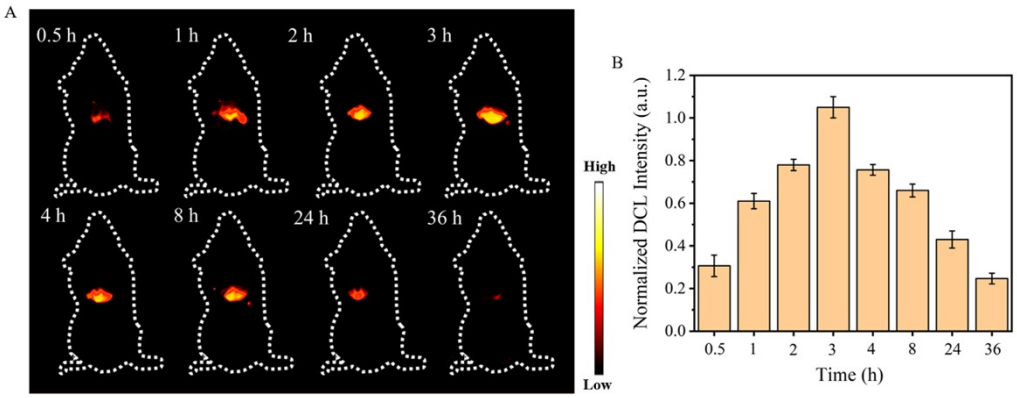

Figure S18. (A) NIR-II luminescence imaging of the mice at different time points after injection of Cy-TP-RENPs. (B) NIR-II luminescence intensity in image (A). NIR-II images were obtained under 980 nm laser excitation with a 1300 nm long-pass filter. All data were presented as mean ± SD (n = 3).

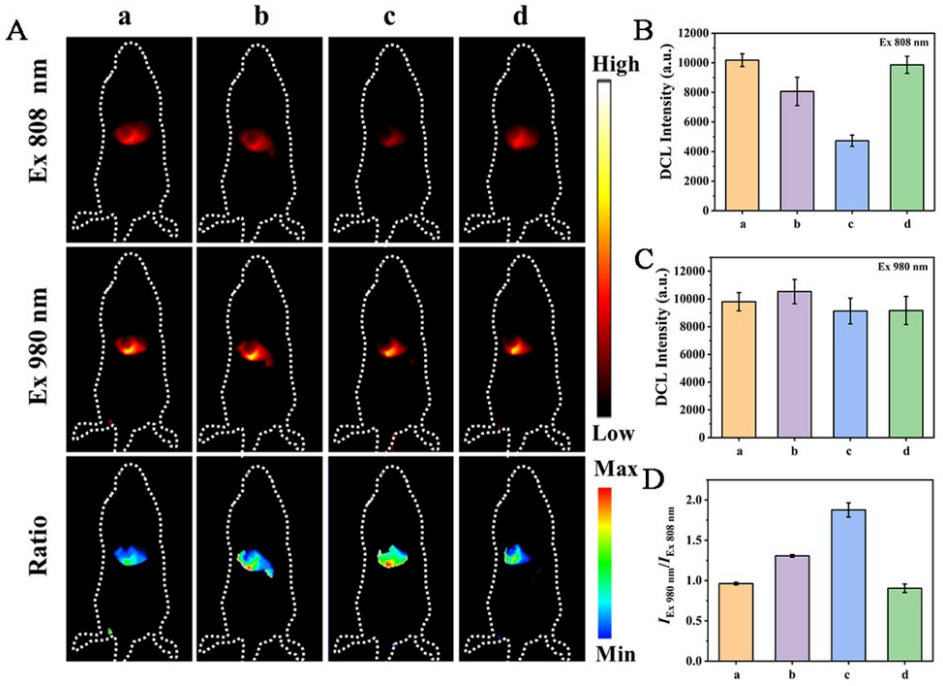

Figure S19. (A) *In vivo* NIR-II luminescence imaging of mice i.p. injected with (a) PBS, (b) GSH (2 mM), (c) AS (25 μg/100 g body weight), (d) AS (62.5 μg/100 g body weight) and (e) AS (62.5 μg/100 g body weight) after i.p. injection with GSH (2 mM) for 1 h. NIR-II luminescence intensities under 808-nm (B) and 980-nm (C) laser excitation in (A). (D) Ratio values ($I_{Ex\ 980\ nm}/I_{Ex\ 808\ nm}$) at the mice liver in (A). All data were presented as mean ± SD (n = 3).

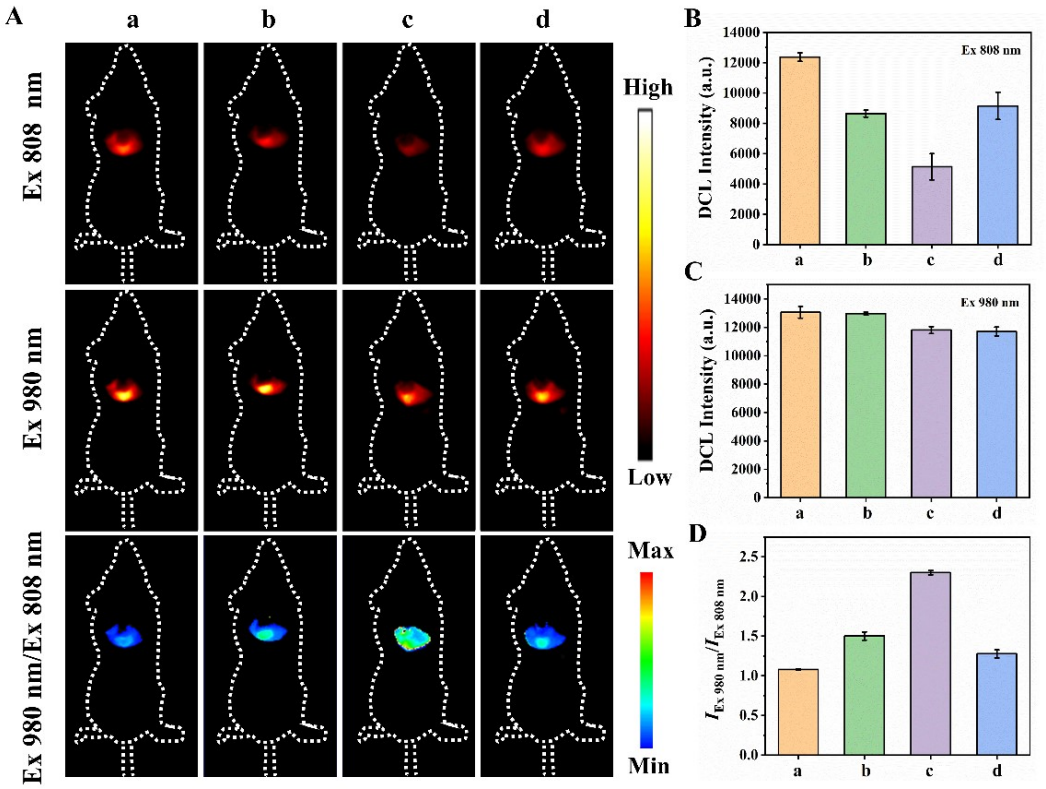

Figure S20. (A) *In vivo* NIR-II luminescence imaging of mice injected with (a) PBS, (b) APAP (10 mg/100 g body weight), (c) APAP (20 mg/100 g body weight) and (d) APAP (20 mg/100 g body weight) after pretreated with α-LA (5 mg/100 g body weight) for 12 h under 808-nm and 980-nm laser excitation. NIR-II luminescence intensities under 808-nm (B) and 980-nm (C) laser excitation in (A). (D) Ratio values ($I_{Ex\ 980\ nm}/I_{Ex\ 808\ nm}$) at the mice liver in (A). All data were presented as mean ±SD (n = 3).

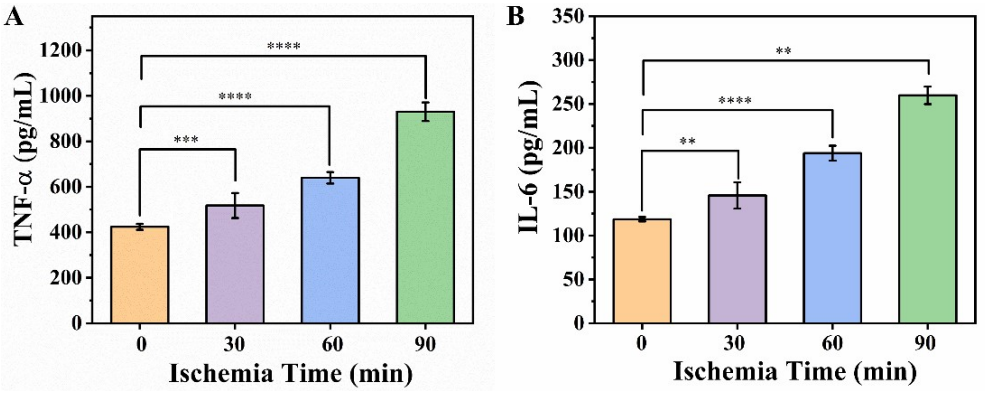

Figure S21. The cytokines TNF-α (A) and IL-6 (B) were detected in liver homogenates from each group via ELISA. Data are represented as the mean ± SD (n=5), **P<0.01, ***P<0.001, ****P<0.0001.

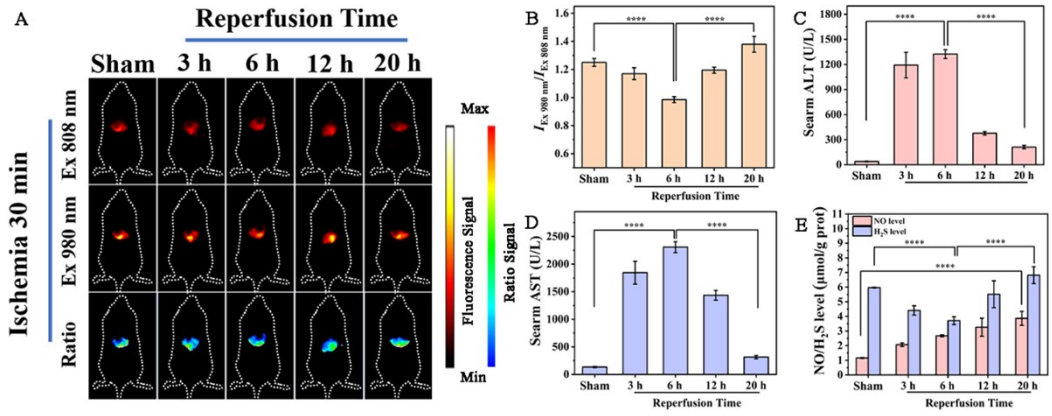

Figure S22. (A) NIR-II luminescence imaging of the mice in sham group (ischemia for 0 min) and IR model group (ischemia for 30 min followed by reperfusion with different time) and corresponding ratiometric imaging. (B) Ratio value ($I_{Ex\ 980\ nm}/I_{Ex\ 808\ nm}$) of the liver regions in (A). Serum ALT (C) and AST (D) levels in the mice of various groups. (E) The amounts of NO and H_2S in mice liver of different groups. All NIR-II images were obtained under 980 or 808-nm laser excitation with a 1300 nm long-pass filter. Data are represented as the mean ± SD (n=5), ****P<0.0001.

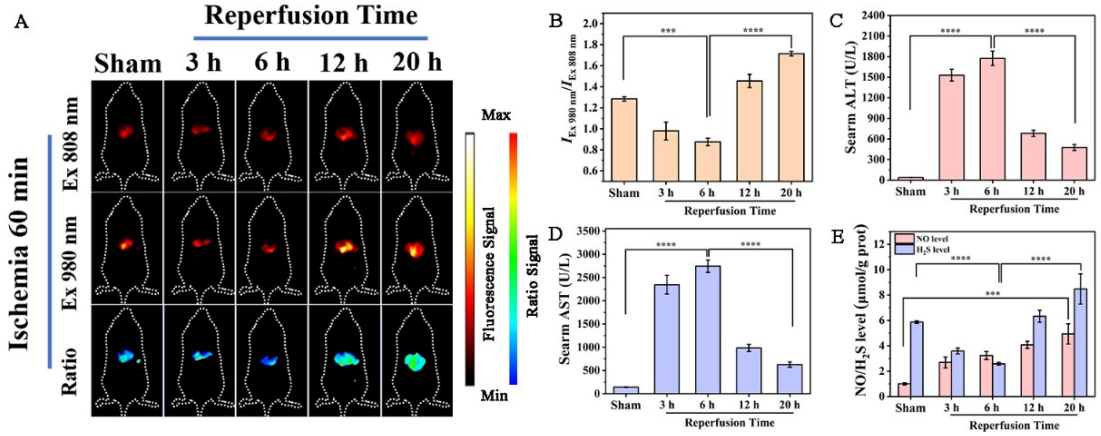

Figure S23. (A) NIR-II luminescence imaging of the mice in sham group (ischemia for 0 min) and IR model group (ischemia for 60 min followed by reperfusion with different time) and corresponding ratiometric imaging. (B) Ratio value ($I_{Ex\ 980\ nm}/I_{Ex\ 808\ nm}$) of the liver regions in (A). Serum ALT (C) and AST (D) levels in the mice of various groups. (E) The amounts of NO and H_2S in mice liver of different groups. All NIR-II images were obtained under 980 or 808-nm laser excitation with a 1300 nm long-pass filter. Data are represented as the mean ± SD (n=5), ***P<0.001, ****P<0.0001.

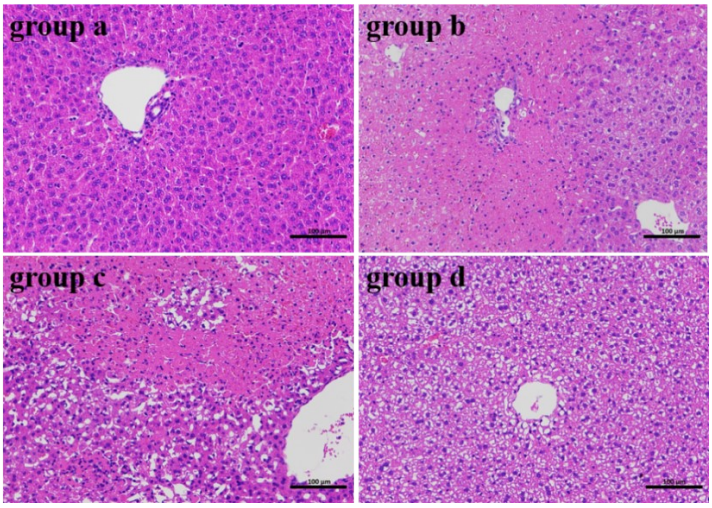

Figure S24. H&E staining of mice hepatic tissues in different groups (a: sham group: ischemia for 0 min; b: IR model mice with 90-min ischemia followed by 24-h reperfusion; c: IR model mice pretreated with 50 μg/100 g body weight of AS; d: IR model mice pretreated with 100 μg/100 g body weight of AS. Scale bar: 100 μm).

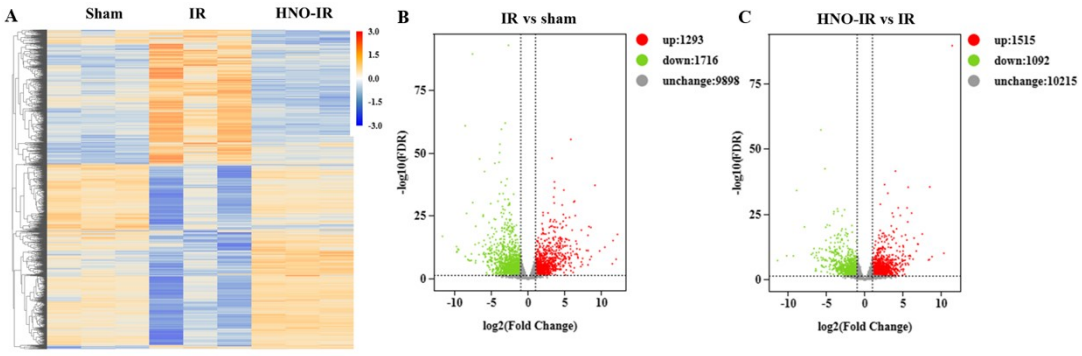

Figure S25. (A) The heat map of genes. Volcano plots showing results of the DEGs in the IR group compared with the sham group (B) and the DEGs in HNO-pretreated IR group compared with the IR group (C). DEGs were identified using Fold change ≥ 2.0 and FDR < 0.05 as the threshold parameters. Down-regulated DEGs are presented as green dots while up-regulated ones are shown as red dots.

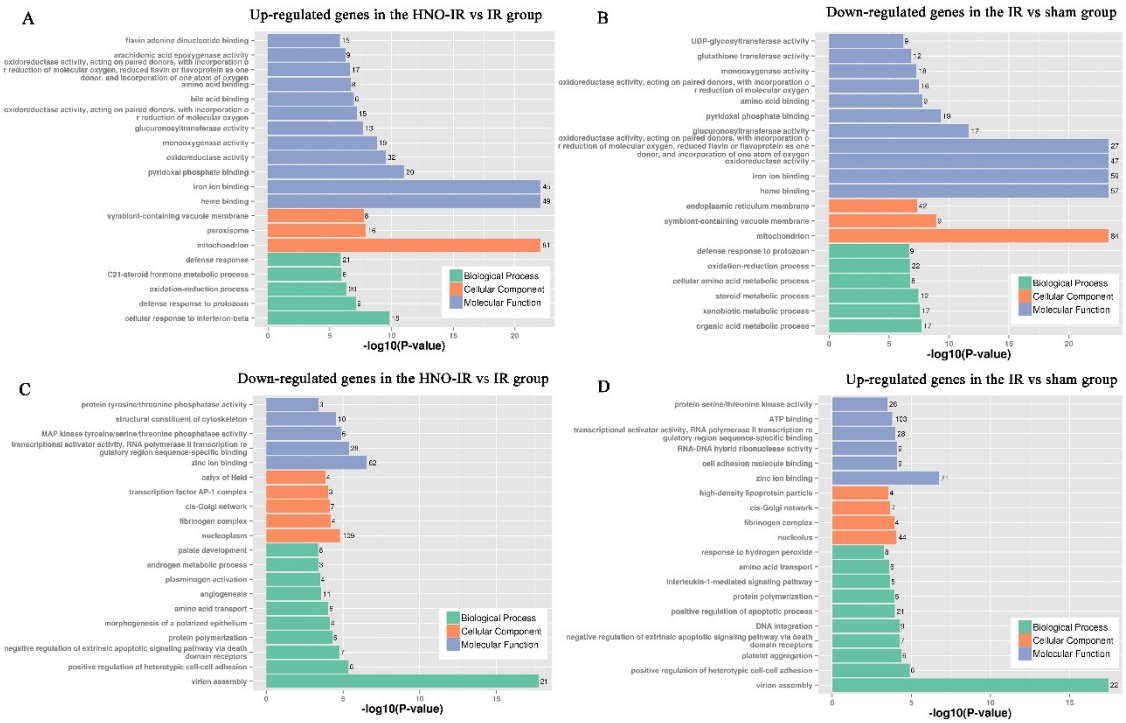

Figure S26. GO terms of up-regulated (A) and down-regulated (C) genes in the HNO-pretreated IR group compared with IR group. GO terms of up-regulated (B) and down-regulated (D) genes in the IR group compared with the sham group.

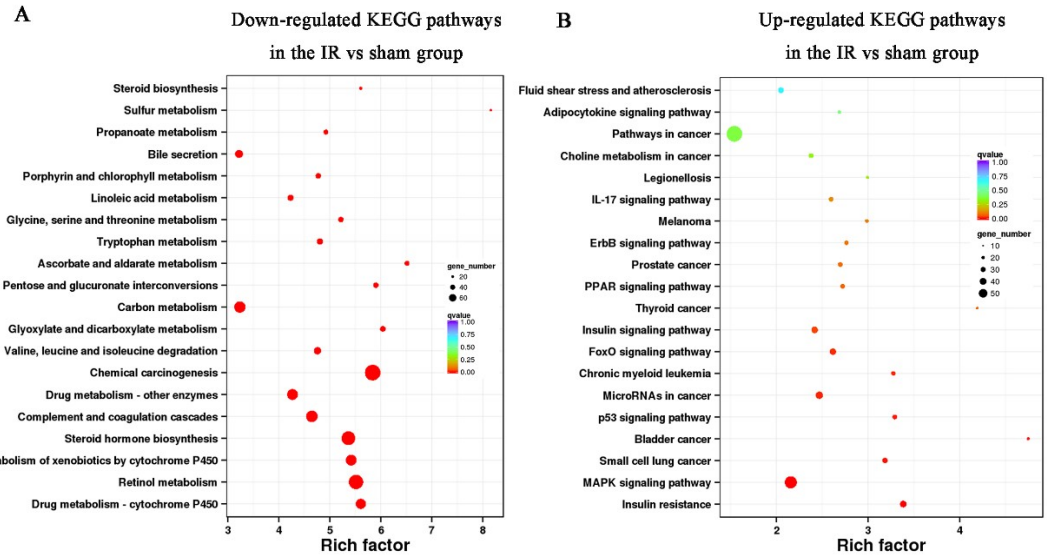

Figure S27. KEGG pathways of up-regulated (A) and down-regulated (B) genes in the IR group compared with the sham group.

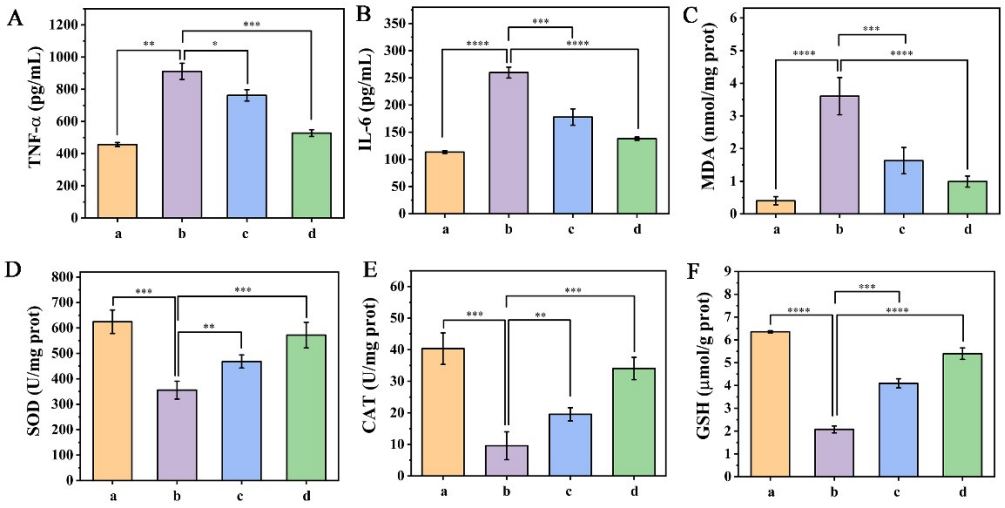

Figure S28. Concentrations of the cytokines (TNF-α, IL-6, panels A, B) and the oxidative stress factors (MDA, SOD, CAT, GSH, panels C–F) in liver homogenates from each group. Data are represented as the mean ± SD (n=5), *P<0.05, **P<0.01, ***P<0.001, ****P<0.0001.

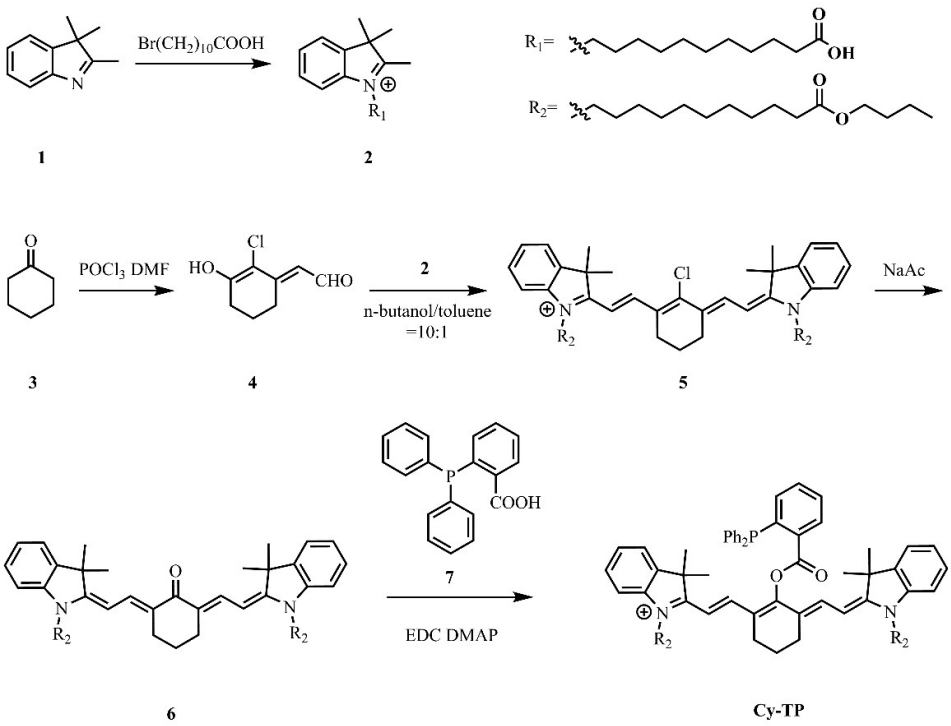

Figure S29. Synthetic route of Cy-TP.

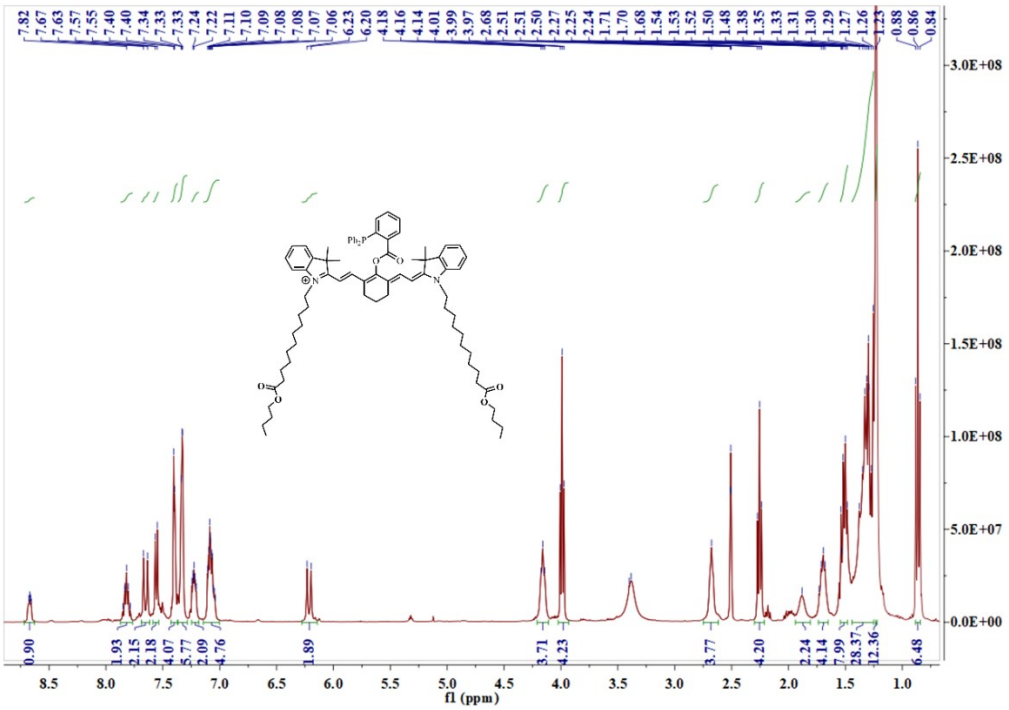

Figure S30. ^{1}H NMR spectrum of Cy-TP.

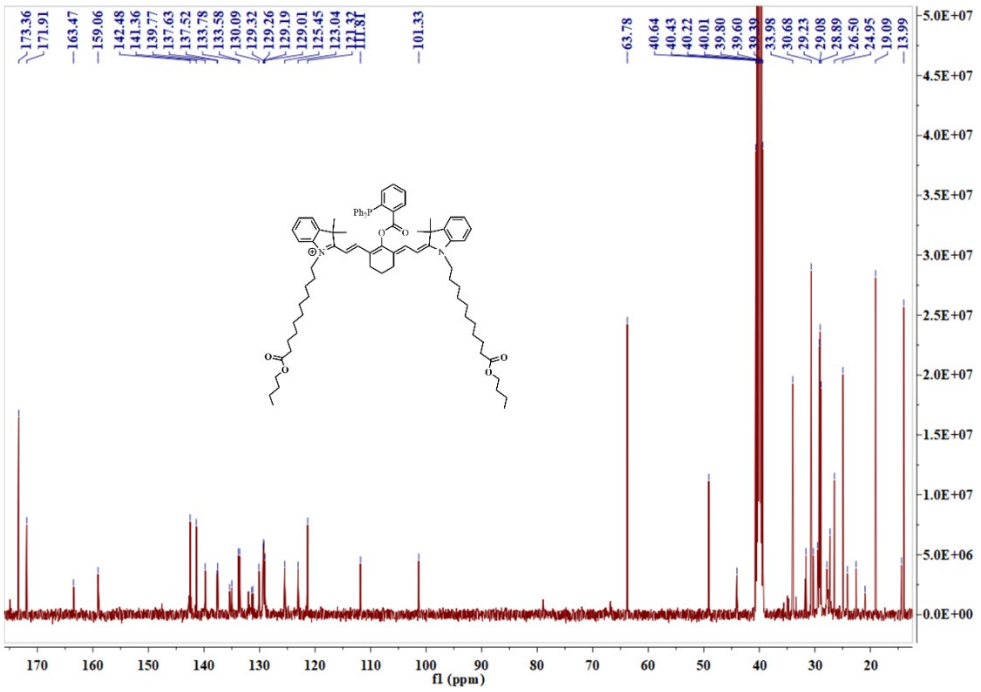

Figure S31. ^{13}C NMR spectrum of Cy-TP.

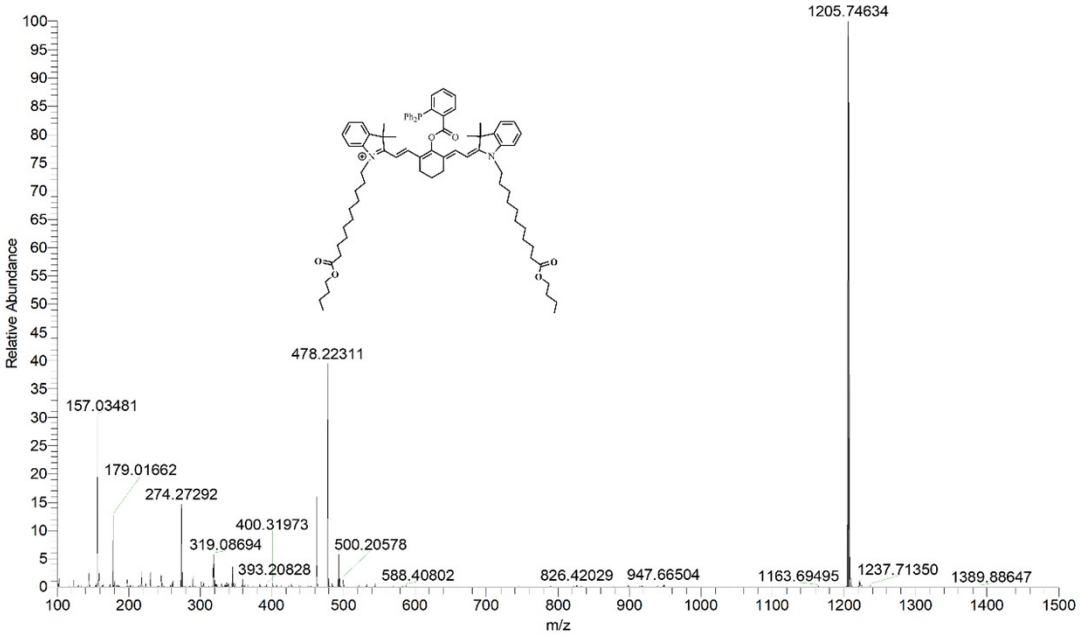

Figure S32. HRMS spectrum of Cy-TP.

Reference

1 X. Luo, R. Wang, C. Lv, G. Chen, J. You and F. Yu, *Anal. Chem.*, 2020, **92**, 1589-1597.

2 Y. Jiang, D. Jin, Y. Li, X. Yan and L. Chen, *Res. Chem. Intermed.*, 2017, **43**, 2945-2957.

3 N. He, S. Bai, Y. Huang, Y. Xing, L. Chen, F. Yu and C. Lv, *Anal. Chem.*, 2019, **91**, 5424-5432.

4 X. Han, R. Wang, X. Song, F. Yu, C. Lv and L. Chen, *Biomaterials*, 2018, **156**, 134-146.